



Indian Journal of Chemistry
Vol. 59A, June 2020, pp. 747-751



Synthesis of Na⁺/Ca²⁺ ions modified TiO₂ xerogels through co precipitation method

K.R Prathyusha & Koliyat Parayil Sreenivasan*

Research & Post Graduate Department of Chemistry, M.E.S Kalladi College, Mannarkkad, Palakkad-678 583, Kerala, India

E-mail: sreenichem@gmail.com

Received 18 June 2019; revised and accepted 22 April 2020

We report a facile method for the synthesis of Na⁺/Ca²⁺ ions modified TiO₂ xerogels by coprecipitation followed by calcination process. The resultant materials are well characterized by powder X-ray diffraction, Raman spectroscopy, ultraviolet-visible diffuse reflectance spectroscopy and high resolution transmission electron microscopy. Presence of sodium and calcium ions can influence the crystallinity of rutile TiO₂. The photocatalytic performances of bare rutile TiO₂ along with modified materials such as Na-TiO₂, Ca-TiO₂, Na-Ca-TiO₂ materials are evaluated by calculating the amount of hydrogen evolved during the photocatalytic decomposition of water under light irradiation. This study will be effective in formulating the effect of alkali/alkaline earth metal ions on the photocatalytic activity of rutile TiO₂.

Keywords: Sol- Gel Synthesis, Coprecipitation, Na⁺/Ca²⁺ Modified TiO₂, Photocatalysis, Water Splitting

Semiconductor photocatalyst has been investigated extensively for light enticed degradation of pollutants, particularly for complete destruction of toxic and nonbiodegradable compounds to carbon dioxide and inorganic constituents¹⁻⁸. Among them, TiO₂ is increasing interest due to its unusual properties like non-toxicity, low cost, chemical inertness, non-photocorrosion, high refractive index and high ultraviolet light absorptivity. Recently, number of studies have been devoted to TiO₂ in many technological applications, such as dye sensitized solar cells¹, photocatalysis², photodegradation³. Generation of hydrogen by photocatalytic splitting of water is an ideal choice for clean fuel generation³⁻⁴. However, the high band gap and fast electron-hole recombination in TiO₂ limits its applications. Therefore, alternative methods are essential for improving the visible light sensitivity of TiO₂ and for reducing electron-hole recombination in TiO₂. It was reported that sensitization of TiO₂ with organic dye, cations or anions, and anchoring of small organic molecule can improve the visible light sensitivity of TiO₂. However, the poor solubility of the organic molecule modified TiO₂⁵⁻⁷ and photodegradation⁸⁻¹⁰ in aqueous environment limits their applications. Therefore, modification of the materials using cations or anions might be useful approach for improving the photocatalytic activity of these materials.

There are numerous studies focused on cation modification in TiO₂ nanostructures¹¹⁻¹⁴. These studies were mainly focused on improving the charge

separation, which led to increase the photocatalytic efficiencies of the materials¹⁵⁻¹⁷. The phase transformation of TiO₂ from anatase to rutile occurs at a temperature range of 450 to 800 °C, which provides better crystallinity and larger crystallite size¹⁸. Moreover, impurities such as metal ions can affect the phase transition as reported earlier¹⁹. The presence of impurities can also influence the photocatalytic properties of the semiconductor materials. However, the photocatalytic properties of alkali/alkaline earth metal ion doped rutile TiO₂ materials were rarely been investigated. In this study, sodium/calcium ions modified TiO₂ photocatalysts are prepared by coprecipitation method. In order to understand the photocatalytic efficiency of the synthesized materials we studied the photocatalytic generation of hydrogen fuel from aqueous suspension of TiO₂ under visible light irradiation in presence of a sacrificial agent. It was found that the photocatalytic activities of the alkali/alkaline earth metal ion modified TiO₂ photocatalysts very much depend on the metal ions used during synthesis.

Materials and Methods

Commercially available titanium tetra isopropoxide, Ti(OPri)₄ (97%, Sigma Aldrich, USA), Ethanol (Nice Chemicals, India), Conc. HNO₃ (Nice Chemicals, India), Sodium Chloride (Nice Chemicals, India) and Calcium Chloride (Nice Chemicals, India) were used.

Typically 2.2 mL of titanium tetra isopropoxide was added drop wise to a solution containing 18 mL

of ethanol under vigorous stirring in a beaker. The hydrolysis process was initiated by the addition of 1 mL water and catalyzed by addition of 100 μ L con. HNO_3 . The resulting mixture was stirred for 3 h to obtain a wet gel. The obtained product was kept for drying at room temperature. After room temperature drying the obtained material was calcined at 550 $^\circ\text{C}$ for 6 h in a static air environment.

Coprecipitation synthesis of sodium ion or calcium ion modified TiO_2 xerogels

To study the role of sodium ions or calcium ions on the formation, structure and activities of TiO_2 xerogel, we prepared sodium and calcium modified TiO_2 materials individually by coprecipitation method. Briefly 1 mL of 2 wt% sodium chloride or calcium chloride solution was added to a stirred solution containing 18 mL ethanol and 2.2 mL titanium tetra isopropoxide solution. 100 μ L conc. HNO_3 was added to the reaction mixture. The resultant mixture was aged for 3 h at room temperature. This led to the formation of a wet gel through condensation process. The obtained material was calcined at 550 $^\circ\text{C}$ for 6 h. The resulting xerogel material was labeled as Na- TiO_2 and Ca- TiO_2 xerogel, respectively.

Coprecipitation synthesis of sodium and calcium ions modified TiO_2 xerogel

To notice the combined effect of sodium/calcium ions in modulating the properties of TiO_2 , we prepared sodium/calcium ions modified TiO_2 material by coprecipitation method. About 0.5 mL of 2 wt% solution of sodium chloride and 0.5 mL of 2 wt% solution of calcium chloride were added to a solution containing 18 mL ethanol and 2.2 mL titanium tetra isopropoxide precursor. Then 100 μ L con. HNO_3 was added to the mixture. The sol so obtained was aged for 3 h at room temperature. This led to the formation of a gel. This material was further calcined at 550 $^\circ\text{C}$ for 6 h in a static air environment. The obtained material was labeled as Na-Ca- TiO_2 xerogel.

Characterization techniques

The synthesized materials were characterized by powder X-ray diffraction (XRD), ultraviolet-visible diffused reflectance spectroscopy (DRS), Raman spectroscopy and high resolution transmission electron microscopy (HRTEM). The powder XRD measurements were performed at room temperature using a Rigaku Miniflex 600 X-ray diffractometer with $\text{Cu K}\alpha$ radiation. The diffractometer was operated at 40 kV and 44 mA and scanned with a step size of 0.02 $^\circ$ at a scan speed of 1 $^\circ$ /min in the range of

10 $^\circ$ to 80 $^\circ$. Raman spectra were measured on a Bruker Optik GmbH spectrometer with a Raman laser (785 nm) as the light source. The unfiltered beam of scattered laser radiation was focused onto the sample through a microscope objective (x50) for an acquisition time of 10 s and repetition of 10x. The UV-visible DRS were recorded by a Jasco V-550 UV-visible spectrophotometer with Jasco model ISV 469 reflection accessory. For the preparation of sample for HRTEM analysis, the representative material Ca- TiO_2 was dispersed in ethanol, and the suspension was sonicated for 1 h. One drop of the suspension was placed on a TEM grid, and allowed to dry overnight. The instrument used for present study features a high-stability goniometer stage specifically tuned for high tilt tomographic applications. A HRTEM (Jeol/JEM 2100) of voltage 200 kV is capable of a spatial resolution of 0.14 nm and can provide images with 2000X – 1500000X magnification by using a multiscan digital camera (camera length 80-2000 mm). LaB_6 is used as the source of radiation.

Photocatalytic hydrogen evolution studies

In order to understand the role of Na^+ , Ca^{2+} and $\text{Na}^+/\text{Ca}^{2+}$ ions together on the photocatalytic activity of TiO_2 xerogel material, we carried out photocatalytic hydrogen evolution studies on the synthesized materials. The experiment was performed in a stainless steel reactor with a side cavity through which hydrogen gas is taken out. Methanol was used as the sacrificial reagent. Typically, 20 mg of the material was suspended in 50 mL solution containing H_2O and methanol in a 4:1 ratio. The suspension was degassed for 30 min with high-purity nitrogen prior to irradiation. The sample was continuously stirred throughout the course of the experiment. A high power mercury arc lamp was used as the visible light source for irradiation and H_2 evolution within a time interval of 1 h was recorded. The experiment was carried out for 5 h. Argon was used as the carrier gas. The amount of H_2 produced was measured by gas chromatograph (Shimadzu Gas Chromatograph GC-2010 PLUS) equipped with a molecular sieve column and a TCD detector and by using a previously calibrated plot.

Results and Discussion

The powder XRD patterns of the TiO_2 , Na- TiO_2 , Ca- TiO_2 and Na-Ca- TiO_2 xerogels are shown in Fig. 1. All the synthesized xerogels exhibited peaks at 27.5 $^\circ$,

36.1°, 39.2°, 41.3°, 44.2°, 54.3°, 56.7°, 62.9°, 64°, 68.9° and 69.8° corresponding to d_{110} , d_{101} , d_{200} , d_{111} , d_{210} , d_{211} , d_{220} , d_{002} , d_{110} , d_{301} and d_{112} plane of rutile phase²⁰. It has been reported that anatase to rutile transformation occurs at a temperature range of 400 to 1200 °C during calcination²¹⁻²². The temperature applied for the present study comes within this range. These support the existence of rutile phase in bare TiO₂, Na-TiO₂, Ca-TiO₂ and Na-Ca-TiO₂. The crystallinity of the rutile phase TiO₂ is reduced in these samples as shown by marked variations in the intensities of the XRD peaks. The variations in intensities are in the order TiO₂>Na-Ca-TiO₂> Na-TiO₂> Ca-TiO₂.

In order to validate the XRD studies, we conducted Raman spectroscopic studies on the synthesised materials. The Raman spectra of TiO₂, Na-TiO₂, Ca-TiO₂ and Na-Ca-TiO₂ xerogels are shown in Fig. 2. The bare TiO₂ xerogel exhibited Raman peaks at 143, 240, 440 and 610 cm⁻¹ corresponding to B_{1g}, E_g and A_{1g} modes of vibration of rutile TiO₂. The Raman peak at 240 cm⁻¹ is known to be the compound vibration peak due to multiple phonon scattering process²³. The E_g mode corresponding to 440 cm⁻¹. It is reported that as temperature increases, this band gets broadened²⁴. Since our samples were calcined at 550 °C, the band at 440 cm⁻¹ is slightly broadened. This broadening is found to be significant for TiO₂ and Ca-TiO₂. In Raman spectra, the E_g mode is mainly caused by the symmetric stretching vibration of O-Ti-O in TiO₂, the B_{1g} mode is caused by symmetric bending vibration of O-Ti-O, and the A_{1g} mode is caused by anti-symmetric

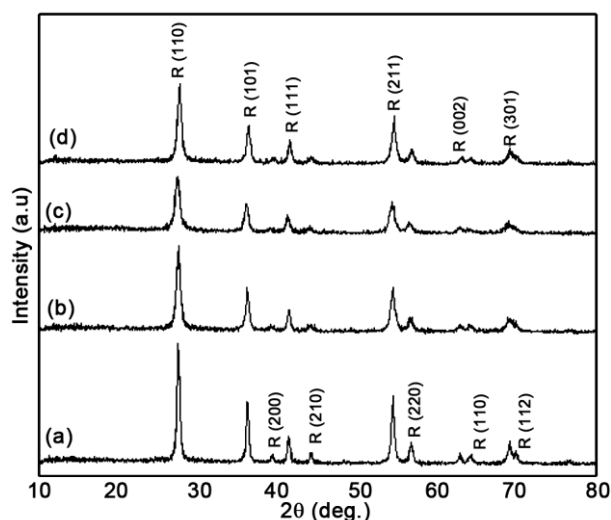


Fig. 1 — XRD Patterns of (a) TiO₂, (b) Na-TiO₂, (c) Ca-TiO₂ and (d) Na-Ca-TiO₂ xerogel.

bending vibration of O-Ti-O²². The samples TiO₂, Na-TiO₂ and Na-Ca-TiO₂ exhibit a weak band at 145.7 cm⁻¹. The intensity of this band is found to be slightly higher for TiO₂ when compared with Na-TiO₂ and Na-Ca-TiO₂. For Ca-TiO₂ this band is absent which may account for its low crystallinity.

To determine the optical properties of the synthesized materials, UV-visible DRS analysis was carried out. The spectra so obtained are shown in Fig. 3. It was reported that the Na⁺/Ca²⁺ ion modified TiO₂ materials exhibited higher absorption wavelength as compared to bare TiO₂²⁵. From the spectrum, it was observed that the absorption wavelength was slightly red shifted for all materials compared to bare TiO₂

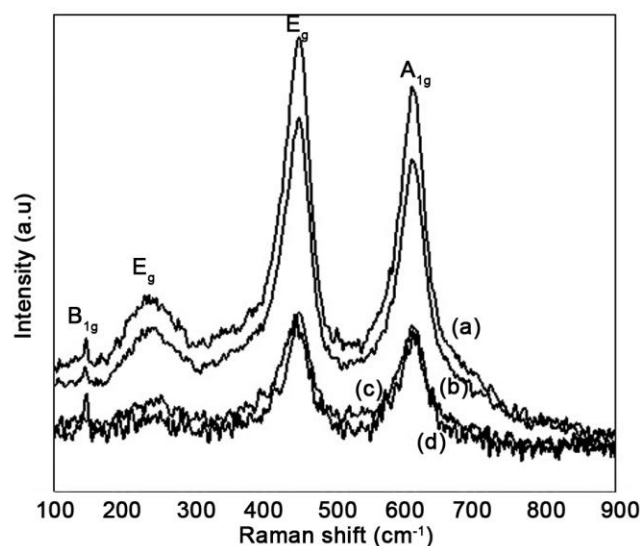


Fig. 2 — Raman spectra of (a) Na-Ca-TiO₂, (b) Na-TiO₂, (c) Ca-TiO₂, and (d) TiO₂ xerogel.

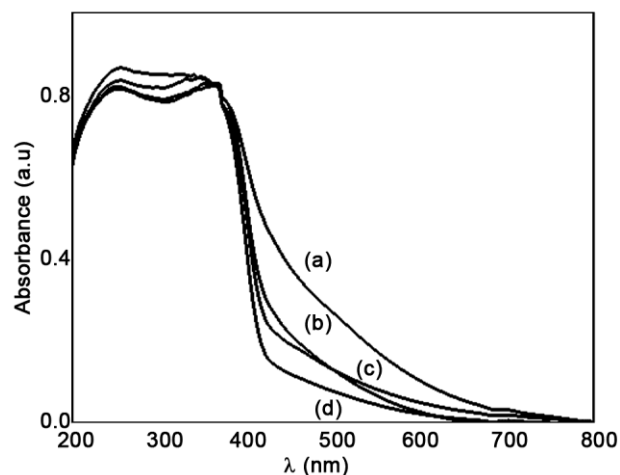


Fig. 3 — DRS spectra of (a) Na-TiO₂, (b) Ca-TiO₂, (c) Na-Ca-TiO₂ and (d) TiO₂ xerogel.

xerogel material. The presence of $\text{Na}^+/\text{Ca}^{2+}$ ions on TiO_2 xerogel causes the absorption band to shift to higher wavelength. Compared to other xerogels, Na-TiO_2 material show high visible absorption wavelength. On the other hand, the sample Ca-TiO_2 and Na-Ca-TiO_2 showed slightly lower absorbance and lower wavelengths when compared with the sample Na-TiO_2 .

The HRTEM image of a representative material Ca-TiO_2 is shown in Fig. 4. From XRD and Raman analysis it is clear that all the synthesized xerogels exhibit rutile phase. The morphological properties of the composites prepared in this study were investigated by collecting HRTEM images of a representative material Ca-TiO_2 . The HRTEM image shows lattice fringes due to rutile TiO_2 ²⁶. The rutile phase with d spacing of 3.25\AA due to R(110) plane could be observed in the HRTEM image.

The photocatalytic H_2 evolution results for bare TiO_2 , Na-TiO_2 , Ca-TiO_2 and Na-Ca-TiO_2 in aqueous suspension with methanol as sacrificial agent (electron donor) are shown in Fig. 5. A high power mercury arc lamp was used as the visible light source for irradiation. It was reported that visible light assisted photocatalytic water splitting is possible for rutile phase TiO_2 ²⁷. Even though the photocatalytic water splitting ability of anatase phase TiO_2 is better than rutile phase TiO_2 under UV light irradiation, the performance of rutile phase TiO_2 is better than anatase under visible light irradiation. From Fig 5, it is observed that the sample TiO_2 showed hydrogen evolution value of $5\ \mu\text{mol}$ after 300 min of visible light irradiation. On the other hand, the samples Na-TiO_2 , Ca-TiO_2 and Na-Ca-TiO_2 showed a value of $1.4\ \mu\text{mol}$, $0.57\ \mu\text{mol}$ and $1.8\ \mu\text{mol}$, respectively. This suggests that the material TiO_2 acquire better photocatalytic activity compared to modified materials. The photocatalytic activities of these materials are in the same order of their rutile phase TiO_2 crystallinity. The relatively high temperature calcination of these materials might promote the phase transition and reduce the surface area of these materials and thereby reducing the hydrogen evolution in photocatalytic water splitting reaction²⁸. The material Na-Ca-TiO_2 , Na-TiO_2 and Ca-TiO_2 do not show H_2 generation until 1 h irradiation. Thus, it is clear that the presence of Na^+ , Ca^{2+} ions reduces the growth of rutile phase and thereby reducing the crystallinity of rutile TiO_2 as indicated by relative peak intensities of rutile TiO_2 in XRD. More over the presence of Na^+ , Ca^{2+} in TiO_2 material may be

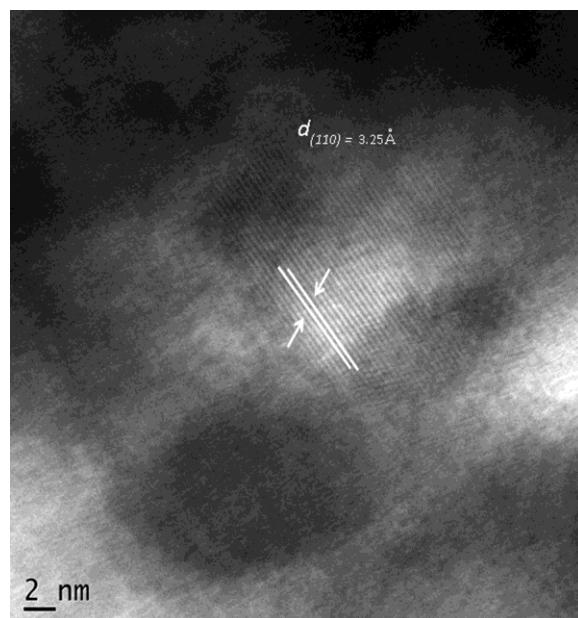


Fig. 4 — HRTEM image of a representative Ca-TiO_2 xerogel material.

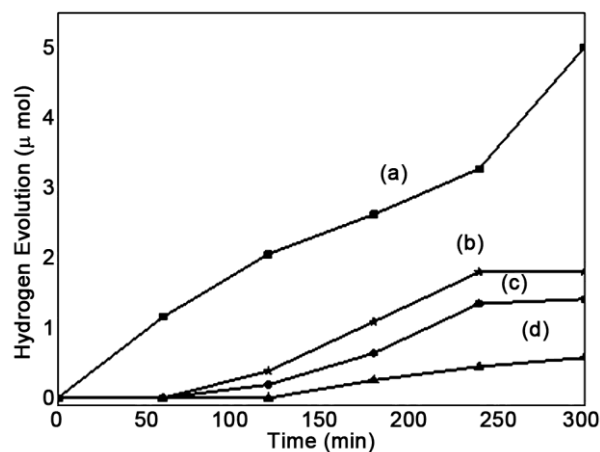


Fig. 5 — A plot of photocatalytic water splitting on (a) TiO_2 (b) Na-Ca-TiO_2 (c) Na-TiO_2 and (d) Ca-TiO_2 .

reducing the catalytic activity of the modified TiO_2 materials as reported earlier²⁹.

Conclusions

We prepared rutile TiO_2 xerogel and sodium and calcium modified TiO_2 xerogels by coprecipitation method. Modification of TiO_2 xerogel material with Na^+ , Ca^{2+} ions reduces the crystallinity of rutile phase TiO_2 . H_2 production from the TiO_2 xerogel material was found to be at the rates as high as $5\ \mu\text{mol}$ from $0.02\ \text{g}$ of catalyst after 30 min of irradiation. However, upon modification with Na^+ and Ca^{2+} or with both of these ions reduced the H_2 production capability of

TiO₂ xerogel materials from 5 -1.4 μmol, 0.57 μmol and 1.8 μmol, respectively. This work provides information for the environmental friendly synthesis of rutile TiO₂ material at relatively low temperature and for understanding influence of alkali/alkaline earth metals on physico-chemical properties of TiO₂ xerogel material.

Acknowledgements

Dr. Parayil acknowledges the financial support of UGC through minor research project grant through 2219-MRP/15- 16/KLCA004/UGC-SWRO.

References

- 1 Hsiao C Y, Lee C L & Ollis D F, *J Catal*, 2 (1983) 418.
- 2 Keiichi T, Kanjana P & Teruaki H, *Water Res*, 34 (2000) 327.
- 3 Rameshwar A, Dileep K & Priyanka, *Acta Chim Pharm Indica*, 4 (2014) 20.
- 4 Sakthivel S, Neppolian B, Palanichamy M, Arabindoo B & Murugesan V, *Water Sci Technol*, 44 (2001) 211.
- 5 Tanmay G & Niladri B, *J Mater Res Technol*, 2 (2013) 10.
- 6 Giah M, Habibi S, Toutounchi S, & Khavei M, *Russ J Phys Chem A*, 86 (2012) 689.
- 7 Ameta R, Vardia J, Punjabi Pinki B & Ameta S C, *Indian J Chem Tech*, 13 (2006) 114.
- 8 Samira B, Amin T Y & Trong O D, *Catal Sci Technol*, 7 (2017) 4548.
- 9 Nakata K & Fujishima A, *J Photochem Photobiol C*, 13 (2012) 169.
- 10 Hagfeldt A, Boschloo G, Sun L, Kloo L & Pettersson H, *Chem Rev*, 110 (2010) 6595.
- 11 Kristine D, Girishkumar G, Vinodgopal K, & Kamat P V, *J Phys Chem B*, 109 (2005) 11851.
- 12 Andraz S, Iztok A, Matjaz M Goran D, Denis A, Pegie C, Urska L S & Natasa N T, *J Mater Chem A*, 6 (2018) 9882.
- 13 Mercedes M & Maroto V, *Appl Catal A*, 502 (2015) 114.
- 14 Sena Y, Hangil L, *Nanoscale Res Lett*, 12 (2017) 582.
- 15 Khairy M & Zakaria W, *Egypt J Petroleum*, 23 (2014) 419.
- 16 Shwetharani R, Sakar M, Fernando C A N, Vassilis B & Balakrishna R G, *Catal Sci Technol*, 9 (2019) 12.
- 17 Song L, Enyan G & Longwei Y, *J Mater Chem*, 22 (2012) 5031.
- 18 Chen Y F, Lee C Y, Yeng M Y & Chiu H T, *J Cryst Growth*, 247 (2003) 363.
- 19 García Serrano J, Gómez-Hernández E, Ocampo-Fernández M & Umapada, *Curr Appl Phys*, 9 (2009) 1097.
- 20 Parayil S K, Kibombo H S, Wu C M, Peng R & Baltrusaitis, *Int J Hydrogen Energy*, 37 (2012) 8257.
- 21 Gouma P I & Mills M J, *J Am Ceram Soc*, 84 (2001) 619.
- 22 Hanaor D A H & Sorrell C C, *J Mater Sci*, 46 (2011) 855.
- 23 Toshiaki O, Fujio I & Yoshinori F, *J Raman Spectrosc*, 7 (1978) 321.
- 24 Guo X Y, Xu D P, Ding Z H & Su W H, *Phys Lett*, 23 (2006) 1645.
- 25 Junqing Y, Guangjun W, Naijia G, Landong L, Zhuoxin L & Xingzhong C, *Phys Chem Chem Phys*, 15 (2013) 10978.
- 26 Choudhury B & Choudhury A, *Int Nano Lett*, 17 (2013) 55.
- 27 Amano F, Nakata M & Ishinaga E, *Chem Lett*, 43 (2014) 509.
- 28 Parayil S K, Kibombo H S, Koodali R T, *Catal Today*, 199 (2013) 8.
- 29 Murat E K, Travis L & Yury G, *Int J Appl Glass Sci*, 2 (2011) 108.